Brain Stimulation 14 (2021) 209–216

Contents lists available at ScienceDirect

Brain Stimulation

journal homepage: http://www.journals.elsevier.com/brain-stimulation

Neuro-cardiac coupling predicts transcutaneous auricular vagus nerve stimulation effects

Marius Keute*, Kathrin Machetanz, Levan Berelidze, Robert Guggenberger, Alireza Gharabaghi**

Institute for Neuromodulation and Neurotechnology, Department of Neurosurgery and Neurotechnology, And Tuebingen NeuroCampus, University of Tuebingen, Tuebingen, Germany

ARTICLE INFO

Article history:
Received 5 October 2020
Received in revised form
24 November 2020
Accepted 4 January 2021
Available online 7 January 2021

Keywords:
Auricular stimulation
Transcutaneous auricular vagus nerve stimulation
Non-invasive vagus nerve stimulation
Heart rate variability
Autonomic nervous system
Parasympathetic nervous system
Neuro-cardiac coupling

ABSTRACT

Background: Transcutaneous auricular Vagus Nerve Stimulation (taVNS) is a non-invasive neuromodulation technique that may constitute an effective treatment for a wide range of neurological, psychiatric, and medical conditions. One key challenge in taVNS research is the high interindividual response variability. To gain an understanding of this variability, reliable biomarkers for taVNS responsiveness would be highly desirable. In this study, we investigated physiological candidate biomarkers while systematically varying stimulation conditions and observing physiological state characteristics.

Methods: Forty-four healthy young adults received taVNS and sham-stimulation. Subjects were pseudo-randomly assigned to stimulation of the left or right ear. Each subject underwent six blocks of stimulation. Across blocks, respiration-locking (inhalation-locked taVNS vs. exhalation-locked taVNS vs. sham) and the electrode location (tragus vs. cymba conchae) were varied. We analyzed heart rate (HR), various heart rate variability (HRV) scores, and neuro-cardiac coupling (NCC), indexed by the relationship between electroencephalographic delta power and heartbeat length.

Results: We observed an effect of taVNS on HR and HRV scores during, but not after stimulation. The direction of the effects was consistent with parasympathetic activation. We did not observe any systematic influence of the stimulation conditions that we varied. However, we found baseline NCC scores to be significant predictors for the individual effect of taVNS on HRV scores.

Conclusion: Cardiac effects of taVNS indicate parasympathetic activation. These effects were short lived, which might explain that some previous studies were unable to detect them. We propose NCC as a novel candidate biomarker for responsiveness to taVNS.

Introduction

Recent years have seen a growing interest in transcutaneous auricular Vagus Nerve Stimulation (taVNS), on the part of both researchers and clinicians. TaVNS holds great promise as a low-risk and low-cost treatment in an impressively wide range of medical fields such as neurology, psychiatry, cardiology. However, empirical findings have been varied, and include a significant proportion of clinical non-responders [21], as well as non-replications of earlier findings [11]. A concerted effort is therefore currently being made to determine biomarkers for taVNS responsiveness, i.e., physiological readouts that can reliably monitor taVNS effects and/or predict whether a subject will respond to taVNS. Any biomarkers that are reproducibly associated with – but not necessarily caused by – the condition of interest [31], could be used to titrate stimulation parameters (i.e., current intensity, pulse width, stimulation frequency), identify optimal stimulation targets within the auricle and/or detect susceptible physiological states, e.g., during the respiratory cycle [10,19,40].

Candidate taVNS biomarkers include cardiac, neurophysiological, and biochemical readouts [10]. Electrocardiographic (ECG) metrics are considered to be among the most promising candidate biomarkers [17,20], for two reasons: Firstly, ECG is inexpensive, and quickly and safely applicable in virtually all patient subpopulations, unlike, for example, magnetic resonance imaging-based

* Corresponding author. Institute for Neuromodulation and Neurotechnology, University of Tuebingen, Otfried-Mueller-Str.45, 72076, Tuebingen, Germany.
** Corresponding author.
E-mail addresses: marius.keute@uni-tuebingen.de (M. Keute), alireza.gharabaghi@uni-tuebingen.de (A. Gharabaghi).

https://doi.org/10.1016/j.brs.2021.01.001

biomarkers [32,45]. Secondly, there is a clear physiological rationale for a relationship between taVNS and cardiac readouts, since the vagus nerve is involved in the autonomic regulation of heart rate (HR), heart rate variability (HRV) and blood pressure (BP) [14,27]. Accordingly, animal studies have confirmed cardiac effects of (invasive) VNS [8,9,13,25,28,29]. Likewise, a growing number of human studies have shown effects of taVNS on HR and HRV, albeit the evidence is less consistent between studies (; [6,17,18,43,44].

This lack of consistency of physiological responses to taVNS could be due to individual trait and state characteristics, such as the auricular innervation pattern [36], pre-stimulation vagal tone [17], or the respiration cycle: a recent study found effects of taVNS on brainstem activations and HRV when taVNS was delivered during exhalation but not during inhalation [40]. In the present study, we aimed to replicate this respiratory dependency of taVNS effects.

Several approaches have been proposed to control for individual baseline characteristics. While methods to map the individual auricular innervation pattern are still under development [26], it is relatively straightforward to take the baseline vagal tone into account, as indexed by ECG metrics [41]. On the other hand, taVNS response variability could be driven by characteristics of the stimulation protocol. To date, a generally accepted standard taVNS protocol does not exist, and stimulation parameters, including current intensity and pulse frequency, appear to exert complex, partly non-monotonic (e.g., U-shaped) and overall elusive influences on stimulation effects [1,7,23,46]. It has also been suggested that various stimulation locations within the auricle may activate different neural pathways, and that the ability to recruit the vagus nerve differs with the stimulation location, given the individual anatomical differences, respectively [12,36,45]. In addition, it has been claimed that taVNS at the left vs. right ear entails different cardiac effects. While no substantial evidence in support of this claim is currently available [16], there is, in general, clear evidence for a lateralization of vagal efferent functions [22,34]. In the present study, we systematically varied the stimulated ear and the electrode location within the auricle to test for an impact on cardiac tavNS effects.

A recent study reported that beat-to-beat HR variations at rest are predicted by EEG delta power around each heartbeat, and that the strength of this association is correlated with HRV indices, suggesting that the coupling between delta power and heart rate can serve as a novel index of (vagally mediated) neuro-cardiac autonomic control [35], thereby rendering it a potentially promising predictor for taVNS responsiveness.

In sum, individual trait and state characteristics as well as characteristics of the stimulation protocol probably contribute to taVNS response variability. The number of different factors that might contribute to taVNS responsiveness, including mutual interactions, highlights the importance of biomarkers in determining the individual optima in this high-dimensional parameter space. In this study, we have three goals: Firstly, we intend to replicate cardiac effects of taVNS so as to further establish them as potential biomarkers. Secondly, we shall examine whether a variation in respiration-locking of taVNS (inhalation-vs. exhalation-locked), stimulation location (tragus vs. cymba conchae), and stimulated ear (left vs. right) systematically modulates cardiac effects of taVNS. Thirdly, we aim to ascertain whether and how the individual pre-stimulation strength of neuro-cardiac coupling (NCC) can predict the individual cardiac response to taVNS.

Methods

Subjects and procedure

Forty-four healthy young [5]adults (M = 28.2 ± 5.6 years of age, 22 females) participated in this study. All were right-handed and had no history of neurological, neurosurgical, or psychiatric, or cardiological disease or treatment (all by self-report). Subjects covered a relatively wide range of height (M = 173.5 ± 8.7 cm; minimum: 160 cm; maximum: 190 cm), weight (M = 69.4 ± 13.8 kg; minimum: 48 kg; maximum: 118 kg) and body-mass indices (BMI, M = 22.9 ± 3.6; minimum: 17; maximum: 39.4).

Subjects were seated comfortably in a reclining chair in a dimly lit room. We prepared various physiological recordings: 59 channel EEG (10-5 montage, 1000 Hz sampling frequency, BrainAmp, BrainProducts GmbH), ECG (two-lead chest montage), electromyography (from several arm muscles, EMG), electrogastrography (EGG), electrooculography (EOG), pupillometry (Pupil Core Eye-tracking Headset, pupil labs GmbH), and respiration (GoDirect respiration belt, Vernier, Inc.) were continuously measured.

Throughout the experiment, participants were at rest, with the instruction to follow a paced breathing rhythm, with 4 s of inhalation, 4 s of exhalation, and 2 s of rest per cycle. Subjects were instructed to focus on their breath, and try to ignore the stimulation. The breathing cycle was visually prompted by a waxing and waning blue circle on the screen, and monitored using a respiration belt (see Fig. 1C). Paced breathing was chosen over free breathing in an aim to control for the number of (respiration-locked) stimulation pulses delivered, and to minimize random fluctuations of respiratory sinus arrythmia (RSA). The experiment was carried out in one session which was divided into six blocks. Across the blocks, stimulation conditions were systematically varied, see section 'Electrical Stimulation'. Each block consisted of a resting physiological measurement (2 min), an intervention (taVNS or sham, 5 min), and a post-intervention resting physiological measurement (2 min). The experiment was approved by the ethics committee of the medical faculty at the University of Tuebingen, and all procedures were carried out in accordance with the Declaration of Helsinki. All participants provided their informed written consent prior to the experiment.

Electrical Stimulation

Electrical stimulation was administered using a handheld bipolar stimulation electrode (Spes Medica Neurotools, see photograph in the Supplementary Material) which delivered rectangular biphasic square pulses with a pulse length of 100 μs and a current intensity (peak-to-peak) of 2 mA. Electrical stimulation was delivered in bursts of five pulses, with a pulse-onset asynchrony of 40 ms (i.e., intra-burst frequency of 25 Hz) and a burst-onset asynchrony of 1 s (i.e., burst frequency of 1 Hz, see Fig. 1B for illustration) using a programmable current stimulator (Multichannel Systems, Harvard Bioscience, Inc.). During the sham conditions, the electrode was held at the cymba conchae or tragus, respectively, but no current was delivered.

Across the six blocks, two stimulation parameters were systematically varied: respiration-locking of stimulation (stimulation during inhalation vs. stimulation during exhalation vs. sham, see

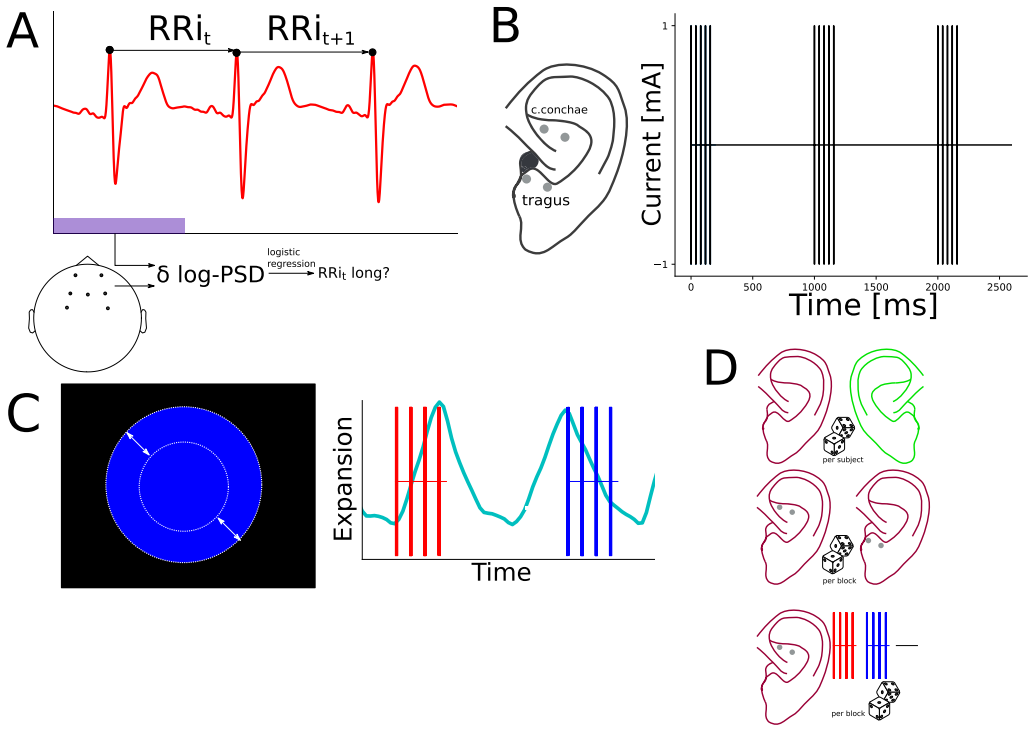

Fig. 1. A: Illustration of the ECG and EEG analysis process. B. Illustration of electrode locations and stimulation protocol. C: Illustration of the visual breathing cue and exemplary respiration belt data. Red and blue vertical lines illustrate stimulation bursts locked to inhalation and exhalation, respectively. D: Illustration of the condition assignment procedure. For each subject, the stimulated ear was selected pseudo-randomly (top row). For each block, electrode location (cymba vs. tragus) as well as respiration locking (red: inhalation-locked, blue: exhalation-locked, black: sham) were selected by pseudo-random permutation. All six possible combinations of location and respiration-locking were conducted with each subject. (For interpretation of the references to colour in this figure legend, the reader is referred to the Web version of this article.)

Fig. 1C), and electrode location (cymba conchae vs. inner tragus auricularis, see Fig. 1B and Supplementary Figures). As an additional between-subject factor, participants were pseudo-randomly assigned to stimulation of the left or right ear (22 subjects each).

Since stimulation was locked to the 4 s periods of inhalation and exhalation, respectively, four bursts were administered per respiration cycle, each followed by a 6-s interval without stimulation. The order of the six blocks was pseudo-randomized across subjects.

ECG data analysis

All HR-related scores were derived from ECG data using the BioSPPy package [15] and custom code written in Python 3. R-peaks were detected automatically and verified by visual inspection. The intervals between successive R-peaks (referred to as RRi, see Fig. 1 A) and instantaneous HR, i.e., the linearly interpolated inverse of RRi, were the basis for the subsequent calculation of all following metrics. We analyzed *mean HR* per subject, condition, and time (pre, stim, post). For statistical analyses, all scores were baseline adjusted to the pre-measurement, see section 'Statistical analyses'. To gain a better understanding about the temporal evolution of stimulation-related HR changes, we visually inspected instantaneous HR over the time course of stim and post. For visualization only (Fig. 2D), we smoothed the HR time course with a 20 s moving-average filter to suppress respiratory sinus arrythmia (see section 'Statistical analyses') and to make any slower HR changes visible. To quantify *RSA*, we averaged instantaneous HR across the paced breathing cycles (10s, starting with the inhalation cue, see Supplementary Figures). Each epoch was mean-centered (to the overall mean of the recording), and multilevel regression models were used to test for an effect of taVNS, as described in the section 'Statistical analyses'. Furthermore, we calculated the following HRV scores: *Root mean squares of successive differences (RMSSD),* i.e., the square root of the mean of squared differences between successive RRi. We also calculated the conceptually similar *Standard deviation of RRi (SDNN).* The *PNN50* score is defined as the percentage of RRi that differs from the preceding RRi by more than 50 ms among all RRi. These *time-domain scores* represent the global beat-to-beat variability of RRi. *Frequency domain scores*, on the other hand, are obtained from a spectral analysis of instantaneous HR. They represent the strength of HR change over a given time window or at a given frequency. We take two frequency domain HRV scores into consideration. *High-frequency HRV (HF)* is the power spectral density (PSD) of HR changes at a frequency between 0.15 and 0.4 Hz. The *LF/HF* score is defined as the ratio between low- (0.04–0.15 Hz) and high-frequency HRV. It is believed to reflect the current balance between sympathetic and parasympathetic activation. Finally, we calculated *SD1/SD2*, a nonlinear HRV score calculated from Poincare recurrence matrices, i.e., a matrix representation of each RRi$_t$ and its subsequent RRi$_{t+1}$. SD1/SD2 is defined as the ratio of the standard deviations of the two principal components of the Poincare recurrence matrix. It provides an estimation of signal unpredictability/complexity [41].

Neuro-cardiac coupling

In accordance with the findings of a recent study [35], we determined the strength of NCC as the relationship between EEG delta power around each R-peak and occurrence of a long vs. short heartbeat. A heartbeat was defined as being long or short if the interval passing between the current and the subsequent R-peak (RRi) was in the upper or lower third of all RRi in the same recording, similar to the methodology described by Ref. [35]. EEG data were bandpass (0.3–35 Hz, 4th order Butterworth filter) and

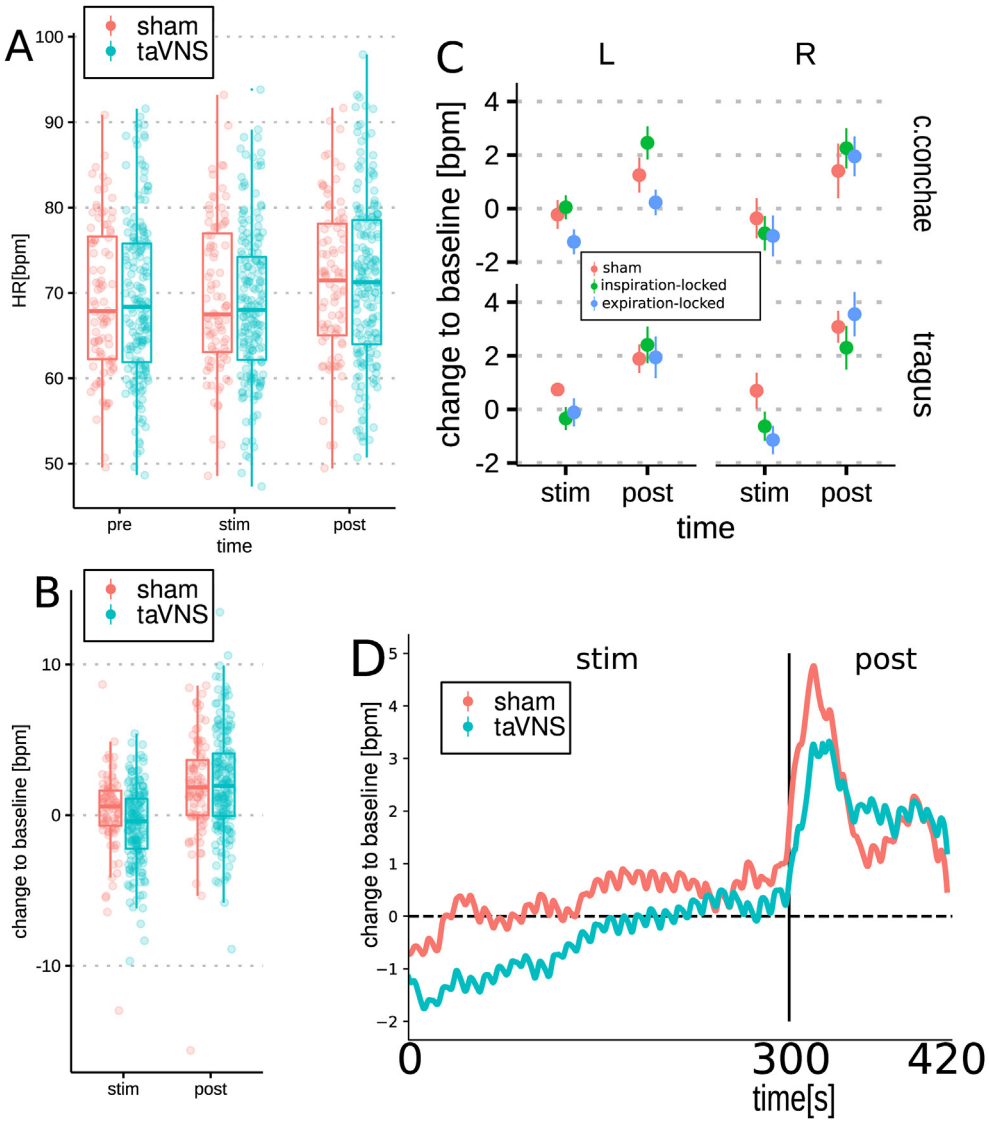

Fig. 2. A. Mean HR per subject, time and condition. B. Change to baseline (pre) in beats per minute. C. Change to baseline, resolved by all fixed factors. D. Change to baseline, time-resolved and moving-average smoothed (window length: 20s). Ripples in the curves are the residual RSA.

notch (48–52 Hz, 4th order Butterworth filter) filtered. Corrupted channels were identified by visual inspection on the basis of intra-channel variance, and excluded from further analysis. Ocular and muscular artifacts were removed using independent component analysis (ICA) based on correlations between the ICA components and the vertical EOG, horizontal EOG, and envelope of the masseter EMG, respectively. To assess NCC, we divided the pre- and post-stimulation EEG data into 1.2 s epochs, starting 0.6 s before each of the R-peaks detected in the simultaneously recorded ECG. Segments with remaining artifacts were excluded on the basis of a threshold criterion (±80 μV). We determined power spectral density (PSD) for each segment using Fast Fourier Transform (FFT) with Hann-tapered windows, zero-padded to a total window length of 2000 samples (2s). PSD values were log-transformed and averaged across delta frequencies (0.5–4 Hz). We defined seven frontocentral electrodes (Fp1, Fp2, F3, F4, Fz, FC3, FC4) as region of interest (ROI), following the results reported by Ref. [35]. Delta power, averaged across the ROI and z-standardized, served as predictor in a logistic model, predicting for each R-peak whether the subsequent R-peak belongs to the lower (short heartbeat) or upper (long heartbeat) third of all RRi. We used the subject-and-condition-wise regression weight, expressed in log-odds per standard deviation, as a measure for the strength and direction of NCC.

Statistical analyses

All scores were analyzed using linear multilevel regression models (LMM) with subject-wise random intercepts and by-subject random slopes for all within-subject effects to account for repeated measurements, i.e., a maximal random effects structure, as is recommended for the procurement of generalizable results [4]. SDNN, RMSSD, HF, LF/HF, and SD1/SD2 were log transformed prior to entering the LMM to approximate normal distributions. PNN50 was converted to log-odds. All scores were baseline-corrected to the respective pre-measurement. Fixed factors were time (on-intervention vs. post-intervention), taVNS (taVNS vs. sham), stimulated ear (left vs. right), electrode placement (tragus auricularis vs. cymba conchae), and a time × taVNS interaction, reflecting an altered time course of HRV in taVNS conditions compared to sham. P-values were calculated from the model F- or t-values,

respectively, using Satterthwaite approximations for (denominator) degrees of freedom. Statistical modeling and testing were carried out in R using the packages lme4 and lmerTest. We conducted post-hoc comparisons by fitting and testing reduced LMM to subsets of the data (e.g., taVNS data only during intervention). To compare baseline characteristics between active and sham blocks, we used non-baseline-corrected values.

Data and code availability

The Python and R code used for data analysis will be made available on Github (https://github.com/mkeute). The data will be available from the corresponding author upon request, as the ethics approval does not allow uploading the datasets to a publicly available repository.

Results

Heart rate

HR changed significantly over time ($F = 41.03$, $p < .001$). Furthermore, there was a main effect of electrode location on HR ($F = 6.42$, $p = .016$), as well as a time × taVNS interaction ($F = 4.54$, $p = .011$), but no main effects of taVNS or stimulated ear (both $F < 0.6$, both $p > .4$). Post-hoc tests revealed that the main effect of time was driven by an increase in HR post-stimulation ($t = 5.16$, $p < .001$), but that HR did not differ significantly from baseline during stim ($t = 0.84$, $p = .403$). Conversely, HR change to baseline was significantly different between sham and taVNS during stim ($t = -2.24$, $p = .030$), but not post-stim ($t = 0.60$, $p = .549$). When considering taVNS data only and separately for stim and post, we found neither main effects of the location or side of stimulation, nor any interaction effects (see Supplementary Results). Baseline HR was not different between sham and taVNS blocks ($t = 0.01$, $p = .992$). Moreover, excluding inhalation locked and exhalation-locked taVNS data, respectively, did not lead to any substantial changes in the pattern of significant effects (see Supplementary Results). Visual inspection of the HR time course (Fig. 2D) revealed that the post-stim HR increase relative to baseline was driven by a transient rebound immediately upon stimulation offset and sham intervention offset, respectively. Furthermore, the relative HR decrease during taVNS was predominantly driven by an HR decrease in the first half of the stimulation period (i.e., about 2.5 min), whereas HR tended to return to the pre-stimulation level in the second half of the stimulation period.

Respiratory sinus arrythmia

Overall, subjects adhered well to the paced breathing rhythm, with a mean phase locking value PLV = .78 ± 0.16 (see Supplementary Methods). Mean RSA (peak-to-peak) during the intervention was 15.59 ± 5.65 bpm (see Supplementary Figures). There were no main effects of condition ($F = 2.02$,$p = .140$), ear ($F = 0.56$, $p = .460$), or of location ($F = 0.210$, $p = .647$) on peak-to-peak RSA, nor did condition interact with ear ($F = 2,30$, $p = .108$) or with location ($F = 1.16$, $p = .316$).

Heart rate variability

The results of the main statistical analysis are summarized in Tables 1 and 2. No main effects of taVNS, location, or ear were found for any of the HRV scores. A significant time × taVNS interaction was, however, found for SDNN, RMSSD, PNN50, HF, and LF/HF, and a marginally significant interaction for SD1/SD2. Much like in HR (see above), we observed that most HRV scores significantly changed over time, across taVNS and sham. Post-hoc comparisons are summarized in Tables 3 and 4. During stimulation, we found the overall (across sham and taVNS) change to baseline to be significantly different from zero for all time-domain HRV scores, HF, and SD1/SD2. Moreover, we found significant differences between sham and taVNS during stimulation for RMSSD, PNN50, and SD1/SD2 (see Fig. 3A). Post-stimulation, we found differences to baseline for some scores, but no significant differences between taVNS and sham. We found no significant effects of respiration-locking, ear or location in the post-hoc comparisons. Baseline HRV scores were not significantly different between sham and taVNS blocks. In addition, the exclusion of inhalation-locked and exhalation-locked taVNS data, respectively, did not lead to any substantial changes in the pattern of significant effects (see Supplementary Results).

Neuro-cardiac coupling

We could not establish any overall trend for a relationship between delta power and heartbeat length at baseline recordings (regression weights were, on the group level, not significantly different from zero, $t = 0.134$, $p = .894$). Neither was NCC different between pre- and post-measurements, i.e., it was unaffected by the intervention ($t = 1.523$, $p = .128$). Finally, baseline NCC did not differ between sham and taVNS blocks ($t = 1.159$, $p = .253$). However, baseline NCC was a significant predictor for the change in SDNN between baseline and taVNS ($t = 3.095$, $p = .002$, see Fig. 3 B), as well as for the change in HF ($t = 2.28$,$p = .024$) and SD1/SD2 ($t = 2.396$, $p = .017$), but not for any of the other HR/HRV metrics (all $|t|<1.65$, $p > .1$). All effects were positive, i.e. a higher (positive) NCC predicted a higher (positive) taVNS effect.

Discussion

Summary and interpretation of findings

In this study, we aimed to corroborate cardiac effects of taVNS, examine the modulation of such an effect by variations in respiration-locking, stimulation location, and the stimulated ear, as well as investigate the potential of individual neuro-cardiac baseline characteristics to predict the responses to taVNS. We identified cardiac taVNS effects, i.e., decreased HR and increased HRV scores RMSSD, PNN50, and SD1/SD2 (but not SDNN, HF, LF/HF), which is consistent with previous findings and, as an overall pattern, reflective of parasympathetic activation [17]. Overall, similar effects

Table 1
F-values for fixed effects.

	HR	SDNN	RMSSD	PNN50	HF	LF/HF	SD1/SD2
time	41.03	2.35	8.69	13.62	4.80	1.05	10.14
taVNS	0.51	0.00	1.17	1.20	0.01	0.20	1.48
location	6.24	0.03	0.17	1.71	0.46	0.04	0.24
ear	0.06	0.30	0.23	0.16	0.00	0.02	0.04
time x taVNS	4.54	3.77	7.24	3.81	5.74	4.52	2.84

Table 2
p-values for fixed effects.

	HR	SDNN	RMSSD	PNN50	HF	LF/HF	SD1/SD2
time	**.000**	.104	**.000**	**.000**	**.011**	.352	**.000**
taVNS	.479	.984	.285	.279	.925	.654	.230
location	**.016**	.870	.680	.197	.499	.840	.624
ear	.806	.587	.630	.695	.953	.880	.837
time x taVNS	**.011**	**.024**	**.001**	**.023**	**.003**	**.011**	.059

Table 3
t-values for post-hoc comparisons.

	HR	SDNN	RMSSD	PNN50	HF	LF/HF	SD1/SD2
taVNS vs. sham during pre	0.01	0.38	−0.72	−0.54	0.2	−0.27	−1.59
taVNS vs. sham during stim	−2.24	1.50	2.68	2.54	1.84	−1.21	2.22
taVNS & sham vs. baseline during stim	0.84	−2.84	−3.77	−3.04	−3.51	1.86	−2.22
taVNS vs. sham during post	0.60	−0.91	−0.68	−0.15	−1.44	1.71	0.02
taVNS & sham vs. baseline during post	5.16	−0.84	−2.72	−3.60	−1.73	−0.14	−2.89

have already been reported, albeit some studies found no cardiac effects of taVNS [10]. This could be due to trait and state characteristics and the stimulation protocol, as detailed in the introduction. We found no effect of taVNS on peak-to-peak RSA.

In accordance with earlier findings, HR changes were visible soon after taVNS onset [24]. No cardiac effects extended beyond stimulation offset. This transient nature of cardiac taVNS effects may provide a further explanation for the inconsistencies between studies. Immediately upon stimulation offset, we detected a HR rebound that occurred across sham and taVNS conditions. This was surprising, since a HR rebound resulting from reinstatement of sympathetic activation after taVNS offset would not be expected to follow the sham stimulation. Very similar findings have, however, already been reported [2], and one possible interpretation is that the HR rebound is partially caused by a cognitive process (e.g., appraisal of the change between intervention and rest). Finally, we demonstrated that the use of a novel stimulation protocol, with intermittent stimulation bursts rather than continuous stimulation at, e.g., 25 Hz, leads to similar cardiac effects as standard taVNS protocols while reducing the overall current delivered.

Moreover, we found no evidence for any systematic difference between inhalation-locked and exhalation exhalation-locked taVNS, which is surprising, since a recent study [40] showed a very prominent influence of taVNS respiration-locking on brainstem activations and HF-HRV, and exhalation-locked taVNS has been used in patient studies for several years [33]. Similarly, we found no evidence that taVNS effects were systematically modulated by variations in stimulation location (tragus vs. cymba conchae) or stimulated ear (right vs left). In sum, none of the stimulation conditions that were varied in this study provided a satisfactory explanation for cardiac response variance. With regard to the stimulated ear, this was anticipated based on anatomical considerations [16] and experimental evidence from left- and right-sided invasive VNS [37].

With respect to stimulation locations (cymba conchae vs. tragus), on the other hand, the question as to whether both targets equally recruit the auricular branch of the vagus nerve is still under debate. In particular, the idea that the cymba conchae is more strongly or more consistently innervated by the vagus nerve than the tragus is mostly based on a single study [36], with partially inconsistent results [12]. Other studies suggest similar vagal innervation patterns for the tragus and cymba conchae [3], and several taVNS studies have shown comparable results for both stimulation targets [3,45], in line with our findings. In sum, the existing evidence supports a similar vagus nerve recruitment at both locations.

Finally, we calculated an index of neuro-cardiac autonomic control that was first described in a recent study [35]. On the group level, we were unable to replicate the reported relationship between EEG delta power and heartbeat length, possibly on account of a slightly different methodology than that used in the original study. In particular, to avoid EEG artifacts of previous or subsequent R-peaks, which could potentially introduce an artifact in the delta frequency range, we used a shorter window length for the spectral analysis (1.2 s rather than 4 s). Importantly, however, we found that individual NCC regression weights predicted stimulation-induced cardiac changes (SDNN, SD1/SD2 and HF). The relationship was positive, i.e., a higher positive NCC at baseline predicted a stronger taVNS effect, which is in agreement with the findings by Ref. [35]; who suggested that a stronger positive NCC reflects a stronger vagally mediated brain-heart communication. Interestingly, we found that NCC was related to SDNN and HF, two of the HRV scores that were not significantly modulated by taVNS on the group level (post-hoc contrast), i.e., where taVNS effects had higher interindividual variability, which in turn can be explained by the NCC. Crucially, NCC did not baseline-to-intervention changes for any HRV metric in the sham condition, i.e., its predictive value was specific to taVNS. In sum, we found tentative evidence that NCC, as assessed by baseline correlations between delta power and heartbeat length, may constitute a promising biomarker for responsiveness to taVNS, even though the precise physiological interpretation of the NCC score and its relationship to taVNS effects warrants further investigation, e.g., with longer baseline recording periods.

Limitations

Our sample size was limited in the light of the experimental design, i.e., our study may well have been underpowered for the detection of subtle effects such as three- and four-way interaction effects between stimulation conditions. The stimulation paradigm that was used in our study (burst stimulation) is novel and has not yet been formally evaluated and compared to other, more established protocols. Moreover, we did not use an active sham condition (e.g., earlobe stimulation), but instead held the electrode at the stimulation sites without delivering current. The somatosensory quality may thus have differed between conditions. We cannot, therefore, fully rule out that the findings may be partially driven by somatosensory or cognitive processes. However, some HRV effects

Table 4
p-values for post-hoc comparisons.

	HR	SDNN	RMSSD	PNN50	HF	LF/HF	SD1/SD2
taVNS vs. sham during pre	.992	.703	.476	.589	.845	.791	.116
taVNS vs. sham during stim	**.030**	.139	**.010**	**.013**	.071	.229	**.031**
taVNS & sham vs. baseline during stim	.403	**.006**	**.000**	**.003**	**.001**	.070	**.029**
taVNS vs. sham during post	.549	.366	.498	.883	.152	.092	.987
taVNS & sham vs. baseline during post	**.000**	.406	**.009**	**.001**	.086	.890	.006

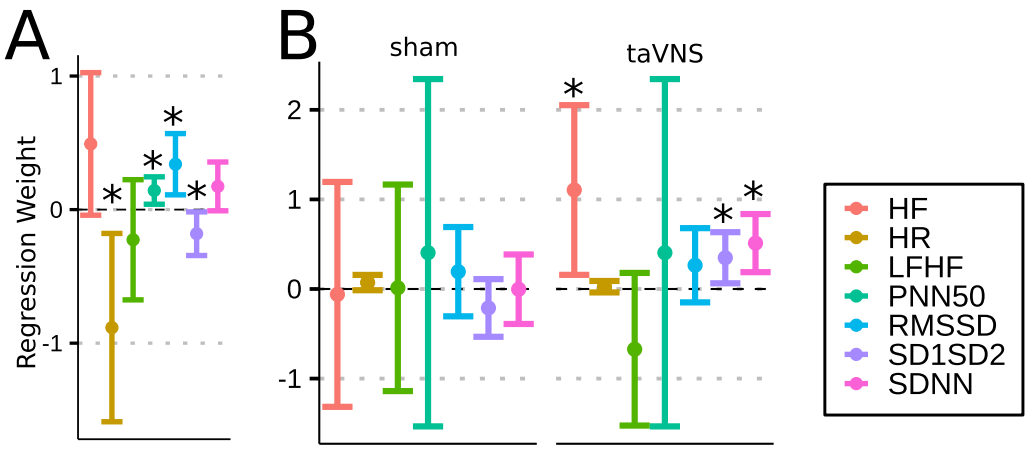

Fig. 3. A. Regression weights and confidence intervals for the taVNS vs. sham post-hoc effect during intervention for all cardiac dependent variables. Significant effects are marked with asterisks. Positive regression weights indicate higher values during taVNS. B: Regression weights and confidence intervals for the prediction of cardiac taVNS effects by baseline NCC. It can be seen that the NCC was a significant predictor for the taVNS effect on HF, SD1/SD2, and SDNN, but for none of the sham effects.

observed during and after the sham condition resembled the findings during the stimulation conditions. This suggests that the applied sham approach was at least sufficient to induce unspecific effects similar to those observed in the stimulation condition. However, taVNS also induced specific HRV effects which did not occur during the sham condition and which were predicted by NCC. Moreover, the paced breathing rhythm used in our experiment might limit the interpretation of frequency-domain HRV scores (HF and LF/HF), since the canonical frequency bands for HF (0.15–0.4 Hz) do not contain the breathing frequency (0.1 Hz). To compensate for this limitation, we conducted an additional analysis of RSA, which is reported in the Supplementary Material. Finally, it is an open question what exactly NCC reflects, in particular with respect to causality, i.e., whether NCC indicates central nervous control of vagal and cardiac function, or rather a cortical response to cardiac changes induced by the autonomous nervous system. Furthermore, the mediating role of physiological covariates, especially respiration, warrant further investigation.

Outlook

It has already been shown that individual patient trait and state characteristics can be predictive of VNS effects, including resting-state brain connectivity [32] and HRV [30]. NCC, as a novel predictive biomarker, has the potential to bridge the gap between the central and autonomic effects of taVNS, branches of research for which no integrative model exists. This might be most relevant for diseases in which a clinical improvement manifests itself in brain and heart functioning alike, e.g., depression [42]. Moreover, a small but growing number of studies on closed-loop taVNS has emerged [38,39], with the aim to optimize the instantaneous autonomic status in real time by coupling taVNS administration to a physiological control signal.

The exact role that NCC could have in this context remains to be determined. In particular, it should be investigated whether intra-individual changes in NCC over longer periods, e.g., several days, reliably predict changes in taVNS responsiveness or whether the NCC-responsiveness relationship that we have reported rather reflects an individual trait that is relatively stable over time. In the latter case, NCC might have a role in selecting patients that are susceptible to taVNS therapy. In the former case, however, NCC could be used as a control signal to, e.g., find the most efficient time windows to deliver taVNS for a given patient. Moreover, it remains an open question whether NCC can be manipulated, e.g., via breathing techniques, and if such a manipulation could enable patients to increase their own susceptibility to taVNS treatment.

Applying taVNS in such a closed-loop fashion requires the availability of wearable measurement and stimulation devices that work in a highly automatized way and that can be easily used by patients. The development of such devices is underway, even though they are not yet available on the market, to the best of our knowledge.

Conclusion

TaVNS, delivered with a burst protocol, led to HR and HRV changes during the stimulation. These effects could be similarly induced at the right and left ear, at the tragus and cymba conchae and during inhalation inhalation and exhalation. Baseline neurocardiac coupling in the EEG delta band may serve as a predictive biomarker for individual taVNS responsiveness; a finding that requires independent replication.

Author contributions statement

MK was responsible for data analysis, interpretation of data, and writing of the manuscript. KM, LB and RB contributed to study design, data acquisition/analysis, and reviewing of the manuscript. AG was responsible for the conception and design of the study, interpretation of data, and writing of the manuscript.

Declaration of competing interest

This research study was supported by the German Federal Ministry of Education and Research [BMBF 13GW0270B, INAUDITAS]. We also acknowledge support by the Open Access Publishing Fund of the University of Tuebingen. None of the authors has potential conflicts of interest to disclose.

Appendix A. Supplementary data

Supplementary data to this article can be found online at https://doi.org/10.1016/j.brs.2021.01.001.

References

[1] Badran BW, Mithoefer OJ, Summer CE, LaBate NT, Glusman CE, Badran AW, DeVries WH, Summers PM, Austelle CW, McTeague LM, Borckardt JJ, George MS. Short trains of transcutaneous auricular vagus nerve stimulation (taVNS) have parameter-specific effects on heart rate. Brain Stimulat 2018;11:699–708. https://doi.org/10.1016/j.brs.2018.04.004.

[2] Badran BW, Brown JC, Dowdle LT, Mithoefer OJ, LaBate NT, Coatsworth J, Bikson M. Tragus or cymba conchae? Investigating the anatomical foundation of transcutaneous auricular vagus nerve stimulation (taVNS). Brain Stimulat 2018a;11(4):947.

[3] Badran BW, Dowdle LT, Mithoefer OJ, LaBate NT, Coatsworth J, Brown JC, George MS. Neurophysiologic effects of transcutaneous auricular vagus nerve stimulation (taVNS) via electrical stimulation of the tragus: a concurrent taVNS/fMRI study and review. Brain Stimulati 2018b;11(3):492–500.

[4] Barr DJ, Levy R, Scheepers C, Tily HJ. Random effects structure for confirmatory hypothesis testing: keep it maximal. J Mem Lang 2013;68:255–78.

[5] Bland JM, Altman DG. Regression towards the mean. BMJ 1994;308:1499.

[6] Borges U, Laborde S, Raab M. Influence of transcutaneous vagus nerve stimulation on cardiac vagal activity: not different from sham stimulation and no effect of stimulation intensity. PloS One 2019;14.

[7] Borland M, Vrana W, Moreno N, Fogarty E, Buell E, Sharma P, Engineer C, Kilgard M. Cortical map plasticity as a function of vagus nerve stimulation intensity. Brain Stimulat 2016;9:117–23.

[8] Brack KE, Coote JH, Ng GA. Interaction between direct sympathetic and vagus nerve stimulation on heart rate in the isolated rabbit heart. Exp Physiol 2004;89:128–39.

[9] Brown GL, Eccles JC. The action of a single vagal volley on the rhythm of the heartbeat. J Physiol 1934;82:211–41. https://doi.org/10.1113/jphysiol.1934.sp003176.

[10] Burger AM, D'Agostini M, Verkuil B, Van Diest I. Moving beyond belief: a narrative review of potential biomarkers for transcutaneous vagus nerve stimulation. Psychophysiology 2020;57:e13571.

[11] Burger AM, Van Diest I, van der Does W, Hysaj M, Thayer JF, Brosschot JF, Verkuil B. Transcutaneous vagus nerve stimulation and extinction of prepared fear: a conceptual non-replication. Sci Rep 2018;8:1–11.

[12] Burger AM, Verkuil B. Transcutaneous nerve stimulation via the tragus: are we really stimulating the vagus nerve? Brain Stimulat 2018;11:945–6. https://doi.org/10.1016/j.brs.2018.03.018.

[13] Buschman HP, Storm CJ, Duncker DJ, Verdouw PD, van der Aa HE. Heart rate control via vagus nerve stimulation. Neuromodulat Technol Neural Interface 2006;9:214–20. https://doi.org/10.1111/j.1525-1403.2006.00062.x.

[14] Capilupi MJ, Kerath SM, Becker LB. Vagus nerve stimulation and the cardiovascular system. Cold Spring Harb Perspect Med 2019:a034173. https://doi.org/10.1101/cshperspect.a034173.

[15] Carreiras C, Alves AP, Lourenço A, Canento F, Silva H, Fred A, et al. BioSPPy - biosignal processing in Python. https://github.com/PIA-Group/BioSPPy/; 2015.

[16] Chen M, Yu L, Ouyang F, Liu Q, Wang Z, Wang S, Zhou L, Jiang H, Zhou S. The right side or left side of noninvasive transcutaneous vagus nerve stimulation: based on conventional wisdom or scientific evidence? Int J Cardiol 2015;187:44–5. https://doi.org/10.1016/j.ijcard.2015.03.351.

[17] Clancy JA, Mary DA, Witte KK, Greenwood JP, Deuchars SA, Deuchars J. Non-invasive vagus nerve stimulation in healthy humans reduces sympathetic nerve activity. Brain Stimulat 2014;7:871–7.

[18] De Couck M, Cserjesi R, Caers R, Zijlstra WP, Widjaja D, Wolf N, Luminet O, Ellrich J, Gidron Y. Effects of short and prolonged transcutaneous vagus nerve stimulation on heart rate variability in healthy subjects. Auton Neurosci 2017;203:88–96. https://doi.org/10.1016/j.autneu.2016.11.003.

[19] Gurel NZ, Huang M, Wittbrodt MT, Jung H, Ladd SL, Shandhi MMH, et al. Quantifying acute physiological biomarkers of transcutaneous cervical vagal nerve stimulation in the context of psychological stress. Brain Stimulat 2019;13(1):47–59.

[20] Gurel NZ, Wittbrodt MT, Jung H, Ladd SL, Shah AJ, Vaccarino V, et al. Automatic detection of target engagement in transcutaneous cervical vagal nerve stimulation for traumatic stress triggers. IEEE J Biomed Health Inf 2020;24(7):1917–25. https://doi.org/10.1101/2020.01.27.20018689.

[21] Hamer HM, Bauer S. Lessons learned from transcutaneous vagus nerve stimulation (tVNS). Epilepsy Res 2019;153:83–4.

[22] Han W, Tellez LA, Perkins MH, Perez IO, Qu T, Ferreira J, Ferreira TL, Quinn D, Liu Z-W, Gao X-B, Kaelberer MM, Bohórquez DV, Shammah-Lagnado SJ, de Lartigue G, de Araujo IE. A neural circuit for gut-induced reward. Cell 2018;175:665–78. https://doi.org/10.1016/j.cell.2018.08.049. e23.

[23] Hulsey DR, Riley JR, Loerwald KW, Rennaker II RL, Kilgard MP, Hays SA. Parametric characterization of neural activity in the locus coeruleus in response to vagus nerve stimulation. Exp Neurol 2017;289:21–30.

[24] Iseger TA, Padberg F, Kenemans JL, Gevirtz R, Arns M. Neuro-Cardiac-Guided TMS (NCG-TMS): probing DLPFC-sgACC-vagus nerve connectivity using heart rate – first results. Brain Stimulat 2017;10:1006–8. https://doi.org/10.1016/j.brs.2017.05.002.

[25] Iwao T, Yonemochi H, Nakagawa M, Takahashi N, Saikawa T, Ito M. Effect of constant and intermittent vagal stimulation on the heart rate and heart rate variability in rabbits. Jpn J Physiol 2000;50:33–9. https://doi.org/10.2170/jjphysiol.50.33.

[26] Kaniusas E, Kampusch S, Tittgemeyer M, Panetsos F, Gines RF, Papa M, Kiss A, Podesser B, Cassara A, Tanghe E, others. Current directions in the auricular vagus nerve stimulation II-an engineering perspective. Front Neurosci 2019;13:772.

[27] Karemaker JM. How the vagus nerve produces beat-to-beat heart rate variability; experiments in rabbits to mimic in vivo vagal patterns. J Clin Transl Res 2015;1:190–204.

[28] Kuo TB, Lai CJ, Huang Y-T, Yang CC. Regression analysis between heart rate variability and baroreflex-related vagus nerve activity in rats. J Cardiovasc Electrophysiol 2005;16:864–9.

[29] Levy MN, Martin PJ, Iano T, Zieske H. Paradoxical effect of vagus nerve stimulation on heart rate in dogs. Circ Res 1969;25:303–14.

[30] Liu H-Y, Yang Z, Meng F-G, Guan Y-G, Ma Y-S, Liang S-L, Lin J-L, Pan L-S, Zhao M-M, Qu W, Hao H-W, Luan G-M, Zhang J-G, Li L-M. Preoperative heart rate variability as predictors of vagus nerve stimulation outcome in patients with drug-resistant epilepsy. Sci Rep 2018;8:3856. https://doi.org/10.1038/s41598-018-21669-3.

[31] Mischak H, Allmaier G, Apweiler R, Attwood T, Baumann M, Benigni A, Bennett SE, Bischoff R, Bongcam-Rudloff E, Capasso G, others. Recommendations for biomarker identification and qualification in clinical proteomics. Sci Transl Med 2010;2:46ps42. 46ps42.

[32] Mithani K, Mikhail M, Morgan BR, Wong S, Weil AG, Deschenes S, Wang S, Bernal B, Guillen MR, Ochi A, Otsubo H, Yau I, Lo W, Pang E, Holowka S, Snead OC, Donner E, Rutka JT, Go C, Widjaja E, Ibrahim GM. Connectomic profiling identifies responders to vagus nerve stimulation. Ann Neurol 2019;86:743–53. https://doi.org/10.1002/ana.25574.

[33] Napadow V, Edwards RR, Cahalan CM, Mensing G, Greenbaum S, Valovska A, Wasan AD. Evoked pain analgesia in chronic pelvic pain patients using respiratory-gated auricular vagal afferent nerve stimulation. Pain Med 2012;13(6):777–89.

[34] Neuser MP, Teckentrup V, Kühnel A, Hallschmid M, Walter M, Kroemer NB. Vagus nerve stimulation boosts the drive to work for rewards. Nat Commun 2020;11(1):1–11.

[35] Patron E, Mennella R, Benvenuti SM, Thayer JF. The frontal cortex is a heart-brake: reduction in delta oscillations is associated with heart rate deceleration. Neuroimage 2019;188:403–10.

[36] Peuker ET, Filler TJ. The nerve supply of the human auricle. Clin Anat 2002;15:35–7.

[37] Premchand RK, Sharma K, Mittal S, Monteiro R, Dixit S, Libbus I, KenKnight BH. Autonomic regulation therapy via left or right cervical vagus nerve stimulation in patients with chronic heart failure: results of the ANTHEM-HF trial. J Card Fail 2014;20(11):808–16.

[38] Romero-Ugalde HM, Le Rolle V, Bonnet J-L, Henry C, Mabo P, Carrault G, Hernández AI. Closed-loop vagus nerve stimulation based on state transition models. IEEE Trans Biomed Eng 2018;65:1630–8.

[39] Romero-Ugalde HM, Rolle VL, Bonnet J-L, Henry C, Bel A, Mabo P, Carrault G, Hernández AI. A novel controller based on state-transition models for closed-loop vagus nerve stimulation: application to heart rate regulation. PLoS One 2017;12:e0186068. https://doi.org/10.1371/journal.pone.0186068.

[40] Sclocco R, Garcia RG, Kettner NW, Isenburg K, Fisher HP, Hubbard CS, Ay I, Polimeni JR, Goldstein J, Makris N, Toschi N, Barbieri R, Napadow V. The influence of respiration on brainstem and cardiovagal response to auricular vagus nerve stimulation: a multimodal ultrahigh-field (7T) fMRI study. Brain Stimulat 2019;12:911–21. https://doi.org/10.1016/j.brs.2019.02.003.

[41] Shaffer F, Ginsberg J. An overview of heart rate variability metrics and norms. Front Publ Health 2017;5:258.

[42] Sperling W, Reulbach U, Bleich S, Padberg F, Kornhuber J, Mueck-Weymann M. Cardiac effects of vagus nerve stimulation in patients with major depression. Pharmacopsychiatry 2010;43:7–11. https://doi.org/10.1055/s-0029-1237374.

[43] Stavrakis S, Humphrey MB, Scherlag BJ, Hu Y, Jackman WM, Nakagawa H, Lockwood D, Lazzara R, Po SS. Low-level transcutaneous electrical vagus nerve stimulation suppresses atrial fibrillation. J Am Coll Cardiol 2015;65:867–75. https://doi.org/10.1016/j.jacc.2014.12.026.

[44] Tobaldini E, Toschi-Dias E, Appratto de Souza L, Rabello Casali K, Vicenzi M, Sandrone G, Cogliati C, La Rovere MT, Pinna GD, Montano N. Cardiac and peripheral autonomic responses to orthostatic stress during transcutaneous vagus nerve stimulation in healthy subjects. J Clin Med 2019;8:496.

[45] Yakunina N, Kim SS, Nam E-C. Optimization of transcutaneous vagus nerve stimulation using functional MRI. Neuromodulat Technol Neural Interface 2017;20:290–300. https://doi.org/10.1111/ner.12541.

[46] Antonino D, Teixeira AL, Maia-Lopes PM, Souza MC, Sabino-Carvalho JL, Murray AR, Deuchars J, Vianna LC. Non-invasive vagus nerve stimulation acutely improves spontaneous cardiac baroreflex sensitivity in healthy young men: a randomized placebo-controlled trial. Brain Stimulat 2017;10:875–81. https://doi.org/10.1016/j.brs.2017.05.006.